U.S. Geological Survey Cooperative Agreement Award Number
Award #G20AP00055

Final Technical Report

# Paleoearthquake Trenching Investigation of the Dog Valley Fault

Ian Pierce (co-PI), Rich D. Koehler (co-PI), and Steve Wesnousky (co-PI)

Nevada Bureau of Mines and Geology
Nevada Seismological Laboratory
Center for Neotectonic Studies

University of Nevada, Reno
1664 N. Virginia St., MS 178
Reno, NV 89557
(775) 682-8763, fax: (775) 784-1709
http://www.nbmg.unr.edu/
ian@nevada.unr.edu
rkoehler@unr.edu
wesnousky@unr.edu

August 30, 2021

Research supported by the U.S. Geological Survey (USGS), Department of Interior, under USGS award number G20AP00055. The views and conclusions contained in this document are those of the authors and should not be interpreted as representing the opinions or policies of the U.S. Geological Survey. Mention of trade names or commercial products does not constitute their endorsement by the U.S. Geological Survey.

**Contents**

**Abstract**
The Dog Valley fault is a left-lateral strike slip fault in the northern Walker Lane. The northern Walker Lane accommodates ~5-7 mm/yr of dextral shear; however, the relative rates of deformation and earthquake history of the Dog Valley fault is poorly characterized. Here, we present geomorphic mapping observations and preliminary paleoseismic trenching results from the Dog Valley fault. Lidar data reveal a clear east-northeast striking fault trace that extends about 25 km from just west of the Polaris Fault near Highway 89 to the northwest flank of Peavine Peak. The lidar data show that the fault goes through Stampede dam. Youthful fault scarps are visible along much of the trace, with alternating (both northwest and southeast) scarp facing directions. Clear lateral displacements are largely absent from the fault, however stepping morphology, sidehill benches, linear valleys and ridges, and alternating scarp facing directions are all consistent with left-lateral strike slip displacement. Stratigraphic and structural relations exposed in the Dog Valley fault trench show clear truncations and tilting of bedded fluvial and peat deposits and provide evidence for the occurrence of at least one Holocene earthquake that postdates ~8 ka. Based on 3D excavations of a prominent channel margin, the most recent earthquake was associated with ~0.8 m of left-lateral displacement.

**Introduction**
The Dog Valley fault in northeast California is a northeast-striking left-lateral strike slip fault that extends for ~25 km from north of Truckee, CA to the north flank of Peavine Mountain near Reno, NV (**Figures 1 and 2**). At this latitude, about 10-15% (5-7 mm/yr) of Pacific/North American plate relative motion (dextral shear) is distributed across the northern Walker Lane with about 2-3 mm/yr concentrated along its western margin (Hammond et al., 2011; Bormann et al., 2013, 2016; Pierce et al., 2021). This deformation is accommodated by active transtensional faulting along the Dog Valley fault as well as a set of conjugate faults including the northwest-striking right-lateral Polaris (e.g., Hunter et al., 2011) and Truckee faults. The system has generated several strong historical earthquakes (1966 M6.6 and two ~M6 earthquakes in 1914 and 1948), numerous smaller earthquakes (e.g. 2021 M4.7), and poses a significant surface fault rupture and strong ground motion hazard for the communities of Truckee, CA and Reno, NV, as well as several water storage dams in the region.

Although the Dog Valley fault is clearly a Quaternary active fault, geologic data on its slip rate, have only been inferred in regional reconnaissance studies (Olig et al., 2005). The previous slip rate estimate for the Dog Valley fault is poorly constrained due to the lack of absolute age control for faulted surfaces and paleoseismic parameters (recurrence, timing of most recent event, etc.) are non-existent. Despite the lack of information on fault rupture parameters, the Dog Valley fault was included in the 2014 update of the U.S. Geological Survey National Seismic Hazard Model (NSHM) with a modeled slip rate of 0.01 mm/yr (Petersen et al., 2014). The Dog Valley fault is anticipated to also be incorporated into the 2023 update of the NSHM (Hatem et al., 2021), however, the fault's rupture behavior remains uncertain. Thus, we initiated a study to better characterize this fault for seismic hazards applications.

**Previous studies along the Dog Valley fault**
The Dog Valley fault is believed to have been responsible for the 1966 M6.6 Truckee earthquake (Reed, 2014). However, features attributed to surface rupture during this earthquake were

described as scattered and discontinuous surface cracking. These features are more likely a result of shaking and may be related to lateral spreading and/or settlement in unconsolidated alluvial deposits, rather than surface rupture along the principal fault trace (Olig et al., 2005). Relocated hypocenters show that the Dog Valley fault forms a distinct lineament of ongoing seismic activity (Reed, 2014). The fault is absent from the geologic map of the Independence Lake and Hobart Mills quadrangles (Sylvester and Raines, 2013).

There are no known peer-reviewed studies published in the last 30 years focused on the Dog Valley fault, however two Bureau of Reclamation (BoR) reports describe several attempts to trench the fault and its general geomorphic character. Hawkins et al. (1986) is the first of these BoR reports. In this study two trenches were excavated to attempt to determine the paleoseismic history of the Dog Valley fault. The first trench was located adjacent to our trench site however their excavation was rapidly filled with water and they did not recognize the fault in the trench. As they did not recognize the fault, the scarp that was excavated was interpreted to be a fault related spring mound. The second trench was not located near a primary strand of the Dog Valley fault, and instead was excavated across a topographic lineament believed to be associated with the 1966 M6.6 Truckee earthquake. Hawkins et al. (1986) described ambiguous stratigraphic relations and did not find compelling geologic evidence for Quaternary offsets in the trench.

The second BoR report is by Olig et al. (2005). In this study they determined that the Dog Valley fault has produced 3.6-4.0 km of cumulative left-lateral offset of the Mafic Andesite flows of Bald Mountain and inferred that this had occurred since ~3 Ma. This implies an average long term left-lateral slip rate of ~1.3 mm/yr. They also described the change in scarp morphology from prominent, primarily northwest-facing scarps along the northeastern portion of the fault zone to alternately facing and more subdued and scattered lineaments along the southwest portion, consistent with our observations from lidar data. Along the fault trace Olig et al. (2005) describe tectonic geomorphic features suggestive of strike-slip motion including side-hill benches, ridge-crest saddles, aligned linear drainages, and reversals in scarp directions. Their report maps and describes a number of other lineaments as part of the Dog Valley fault zone, especially in the area south-southwest of the Stampede Dam. However, these lineaments are omitted from Figure 2 for clarity and only the faults that form the most prominent trace in the lidar imagery (mapped in this project) are shown. The apparent wider distribution of fault traces and lineaments in the southwestern portion of the fault zone described by Olig et al. (2005) may be a result of interactions with the nearly orthogonal Polaris fault, and thus our trenching (box labeled DV1, **Figure 2**) focused on the better-defined singular trace that forms the northeastern portion of the fault zone.

Elsewhere in the Truckee Basin, the northwest-striking right-lateral Polaris fault has been the focus of several studies (Hunter et al., 2011; Melody et al., 2012). The Polaris fault has produced Holocene earthquakes and has a minimum right-lateral slip rate of ~0.4 mm/yr (Hunter et al., 2011). The trenching study by Melody et al. (2012) constrained the timing of the most recent Holocene earthquake on the Polaris fault to <7000 yr B.P., based on displacement of the Tsoyawata (Mazama) tephra. Melody et al. (2012) also documented evidence for an additional late Pleistocene event at the site. The Polaris fault intersects the southwestern end of the Dog Valley fault with a nearly orthogonal geometry (**Figure 2**). Sharp southeast facing fault scarps in glacial outwash deposits along Prosser Creek that fall on-strike with the Dog Valley fault are visible in the lidar data to the southwest of this apparent intersection **(Figure 2**). Olig et al. (2005) also mapped a Truckee fault zone within the basin, which is not the subject of any other known published paleoseismic studies. However, traces of the Truckee fault zone were mapped in greater detail on geologic maps (Sylvester and Raines, 2013) and lidar (Hunter et al., 2011). These studies indicate both normal and right-lateral displacements of glacial moraines along the

Truckee fault zone. Other nearby regional faults include the Mohawk Valley fault to the north (e.g., Gold et al., 2014) and the West Tahoe fault to the south (e.g., Pierce et al., 2017) (**Figure 1**).

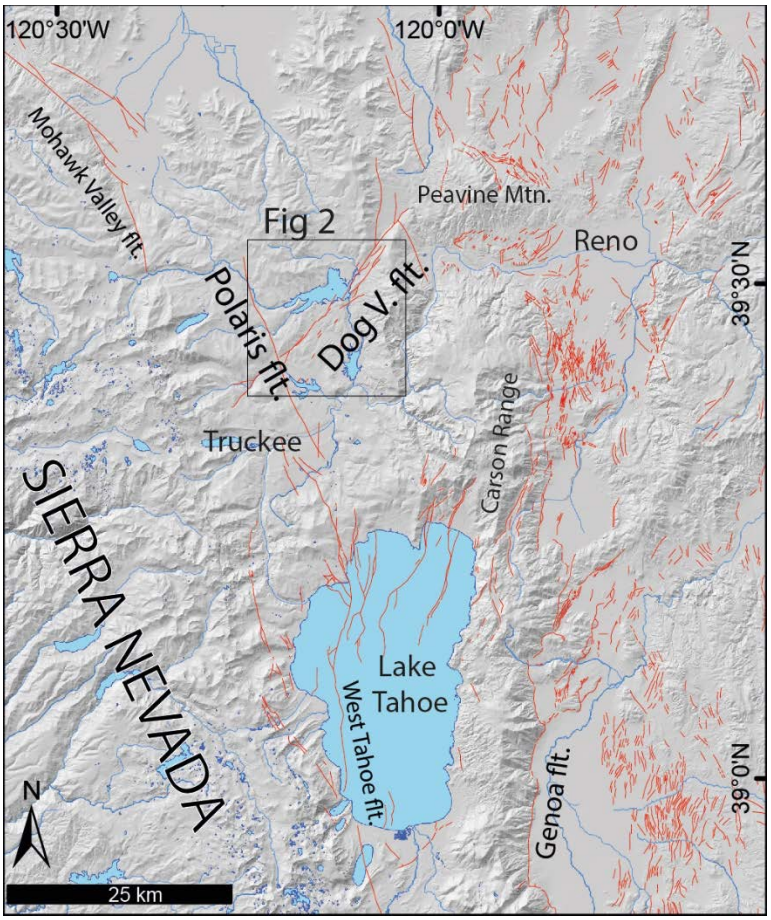


**Figure 1.** *Overview map of the Truckee Basin and surrounding region. Faults in red modified after the USGS Quaternary Fault and Fold Database.*

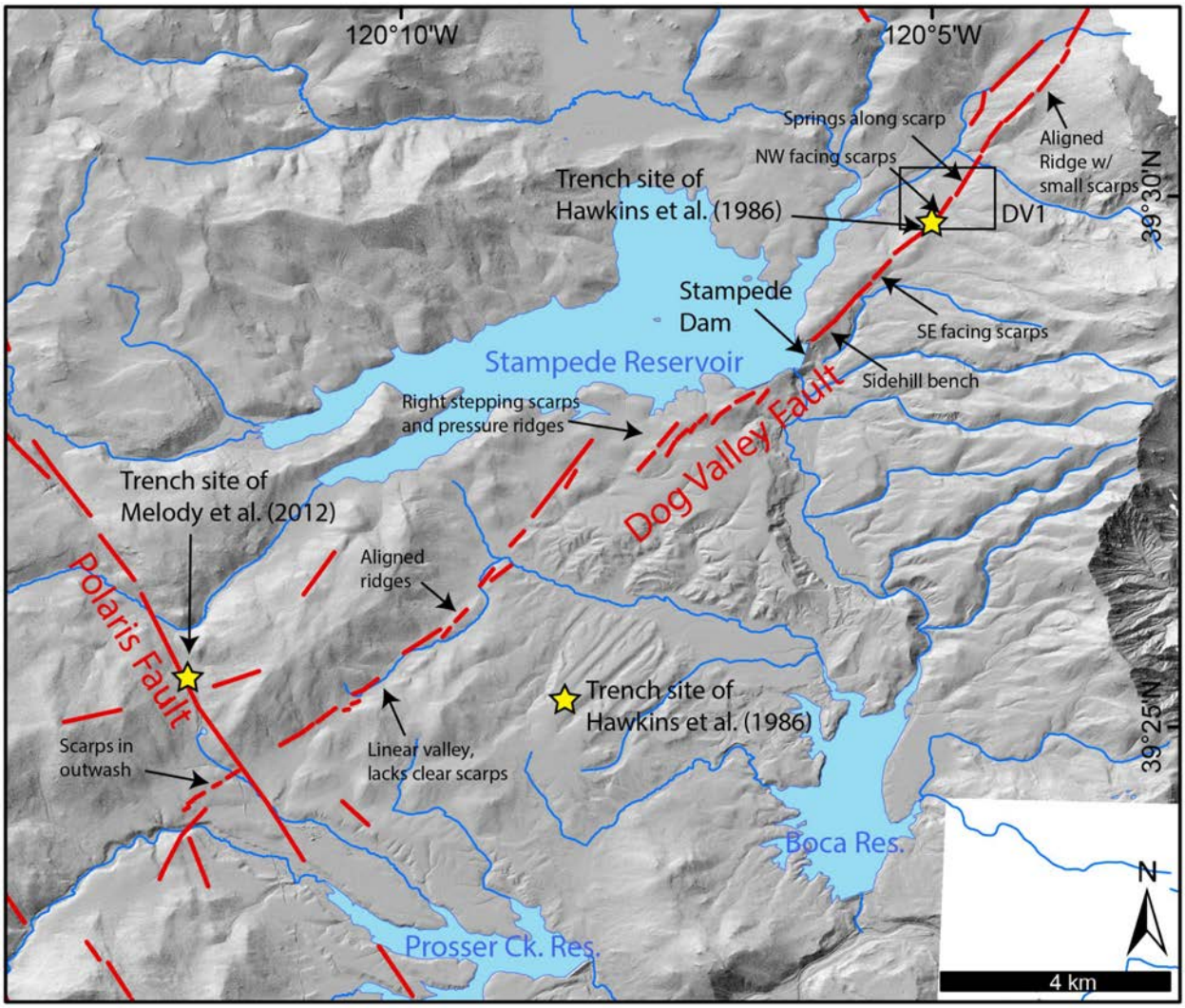


**Figure 2.** *Overview map of the Dog Valley fault. Basemap is a lidar hillshade. Observations of tectonic geomorphology along the Dog Valley fault are indicated by black arrows. Black rectangle shows the location of trench site DV1 adjacent to the trench excavated by Hawkins et al. (1986).*

## Methods

### Trenching

A small excavator remained on site for the duration of the project. After initially logging the first cut of the trench, the excavator was used to progressively peel back trench walls, ~20 cm at a time, creating both fault-parallel and fault-orthogonal slices. Each trench slice was scanned using a 2020 iPad Pro lidar scanner with the SiteScape app and photographed using overlapping photos from a Google Pixel2 smartphone camera. The photos were used to construct SfM models using Agisoft Meatshape software. The dense colored point clouds from the SfM models were then exported into CloudCompare software. In CloudCompare, first all lidar scans were referenced together using flags on the walls in areas of the trench that did not change during progressive excavation as tie points. Then, the SfM point clouds were referenced to each of the corresponding lidar scans, again using flags or small stones in each of the lidar and SfM clouds as tie points.

The final result is a single high resolution spatially accurate 3D model of all 14 trench slices (**Figures 3 and 4**).

**Figure 3.** *Photo of the 3D trench mid-excavation (top). Similarly oriented aligned lidar scans (middle) and higher resolution SfM point cloud (bottom) fitted to the lidar scans. The dotted white lines in the lower scene shows the channel margins that are left-laterally displaced ~80 cm by the fault (dashed red).*

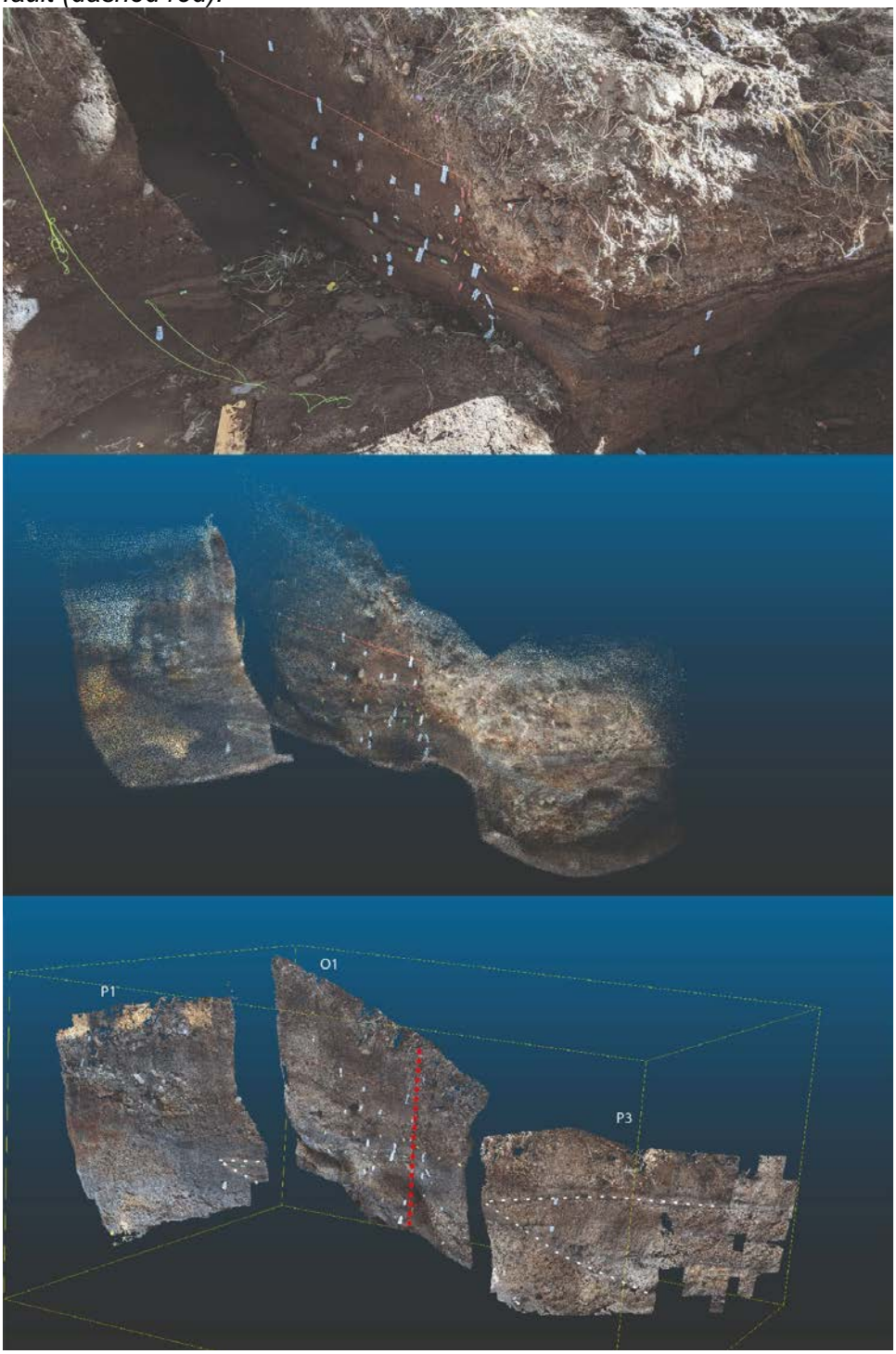

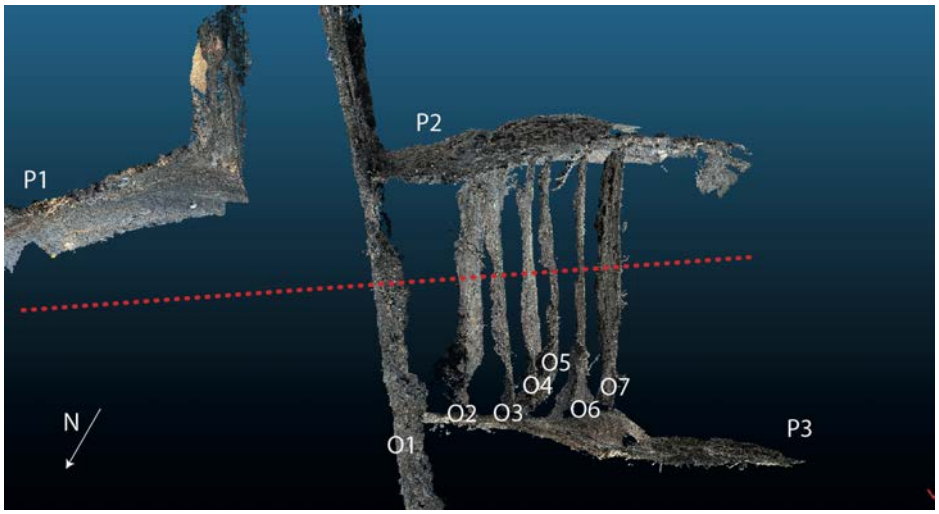


**Figure 4** *Plan view of CloudCompare scene showing the referenced point clouds of 10 of the 14 slices. Fault approximate location dashed in red.*

## Results

### Mapping observations

Tectonic geomorphic features and fault traces were mapped along the length of the Dog Valley fault based on interpretation of lidar hillshade maps and field reconnaissance. This fault linework is provided as a downloadable shapefile (Appendix 3). The main trace of the Dog Valley fault manifests quite clearly in the 2014 Tahoe National Forest lidar imagery (OpenTopography, 2017). Mapping along the Dog Valley fault indicates that it is characterized by right-stepping en echelon fault strands expressed by subdued geomorphic features including both northwest and southeast facing scarps, closed depressions, aligned linear ridges, springs, and sidehill benches (**Figure 2**).

The northeasternmost part of the fault cuts across the northwestern flank of Peavine Mtn. near Reno, NV (**Figure 1**). Southwest from here the fault forms a sharp sidehill bench and aligned ridge before entering Hoke Valley (**Figure 2**). In Hoke Valley, the fault forms a series of springs and 1-2 m high northwest facing scarps along the base of the rangefront bounding the southeastern margin of the valley. At the southwest margin of Hoke Valley, the fault cuts across topography forming a series of linear ridges, sidehill benches, and both northwest and southeast facing scarps before approaching the Stampede Reservoir Dam, maintained by the US Bureau of Reclamation.

The lidar data reveal that the trace of the Dog Valley fault is expressed by a sidehill bench and shallow closed depression immediately northeast of the Stampede Reservoir Dam and appears to project through the footprint of the Dam. Field observations indicate that strands of the Dog Valley fault offset Miocene andesite flow breccias and tuff breccias exposed in a roadcut immediately northeast of the dam (**Figure 5**). Thus, future fault rupture may pose potentially severe, and underappreciated seismic hazard for the downstream communities including Reno, Nevada.

Southwest of Stampede Dam, the fault has a clear right-stepping en-echelon pattern and is expressed by sharp scarps and linear pressure ridges. The fault then continues along a linear ridge and valley, however from here the scarps are less clear and we were unable to precisely locate the fault in the field. Just west of the Polaris fault and Highway 89, the fault is expressed

by a clear southeast facing scarp in glacial outwash deposits along Prosser Creek before terminating into a zone of variably oriented geomorphic lineaments of unknown origin.

A paleoseismic trench (DV1) was excavated approximately 3 km northeast of Stampede Reservoir where the fault forms a 2 m high northwest facing scarp across the mouth of a small alluvial valley (**Figures 2 and 6**). An apparent left deflection of an ephemeral stream channel adjacent to the trench occurs across the fault at this site.

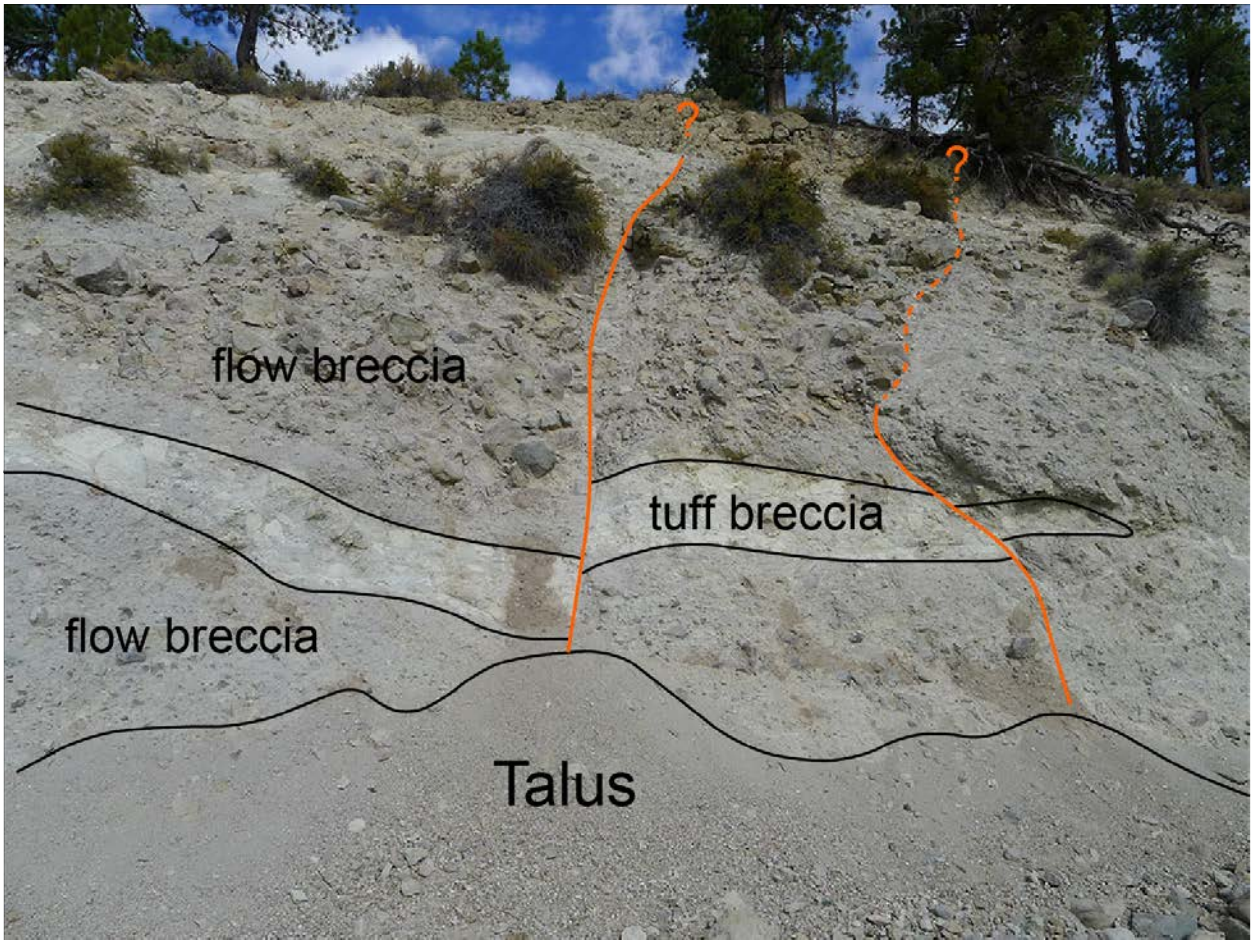


**Figure 5** *Outcrop of faulted volcanic tuffs exposed by roadcut adjacent to east side of Stampede Dam.*

**Hoke Valley trench site (DV1)**

The trench exposed a sequence of low energy saturated interbedded fluvial overbank sands with cobble lenses and peaty buried meadow soils (Units 3 and 4). These deposits are clearly juxtaposed against relatively higher energy dry indurated fluvial course sandy silt and gravel channel deposits (Units 5 and 6) (**Figure 7**). A massive to weakly stratified brown gray silt (Unit 2) and the modern soil (Unit 1) overlies these deposits. Complete descriptions of the units exposed in the trench as well as the soil developed into them are provided in Appendices 1 and 2, respectively. The stratigraphic relations indicate the occurrence of at least one earthquake that broke the entire stratigraphic package. Radiocarbon analyses on 5 charcoal samples (Table

1) constrain the age of the earthquake to after ~8,100 cal yr. BP (samples and ages shown on trench log, **Figure 7**). Several upward fault terminations were observed lower in the stratigraphy however, the similarity of deposits and the flooded conditions at the base of the trench precluded confidently attributing these features to additional paleoevents. A fault parallel slice of the trench (P2 on **Figure 4**) exposed a sand dike (**Figure 8**) that nearly reached the surface, demonstrating limited post-faulting deposition, and precluding dating any post-event deposit that could bracket the age of the event.

The observed facies and thickness changes of stratigraphic units across the fault are consistent with strike-slip displacement. Thus, to assess the amount of lateral displacement in the most recent event, we expanded trench DV1 by cutting fourteen parallel and perpendicular slices of the wall to track a prominent channel margin. The 3D trench scene was used to reconstruct the offset channel margin. The model reconstruction confirmed field measurements indicating that the channel intersects the fault at a high angle and was left-laterally displaced during the most recent earthquake by ~80 cm (**Figure 3**).

**Figure 6.** *Upper: Photo of excavator at the toe of the fault scarp. Lower: east wall of the trench showing sharp juxtaposition of fluvial units across an apparently dipping fault.*

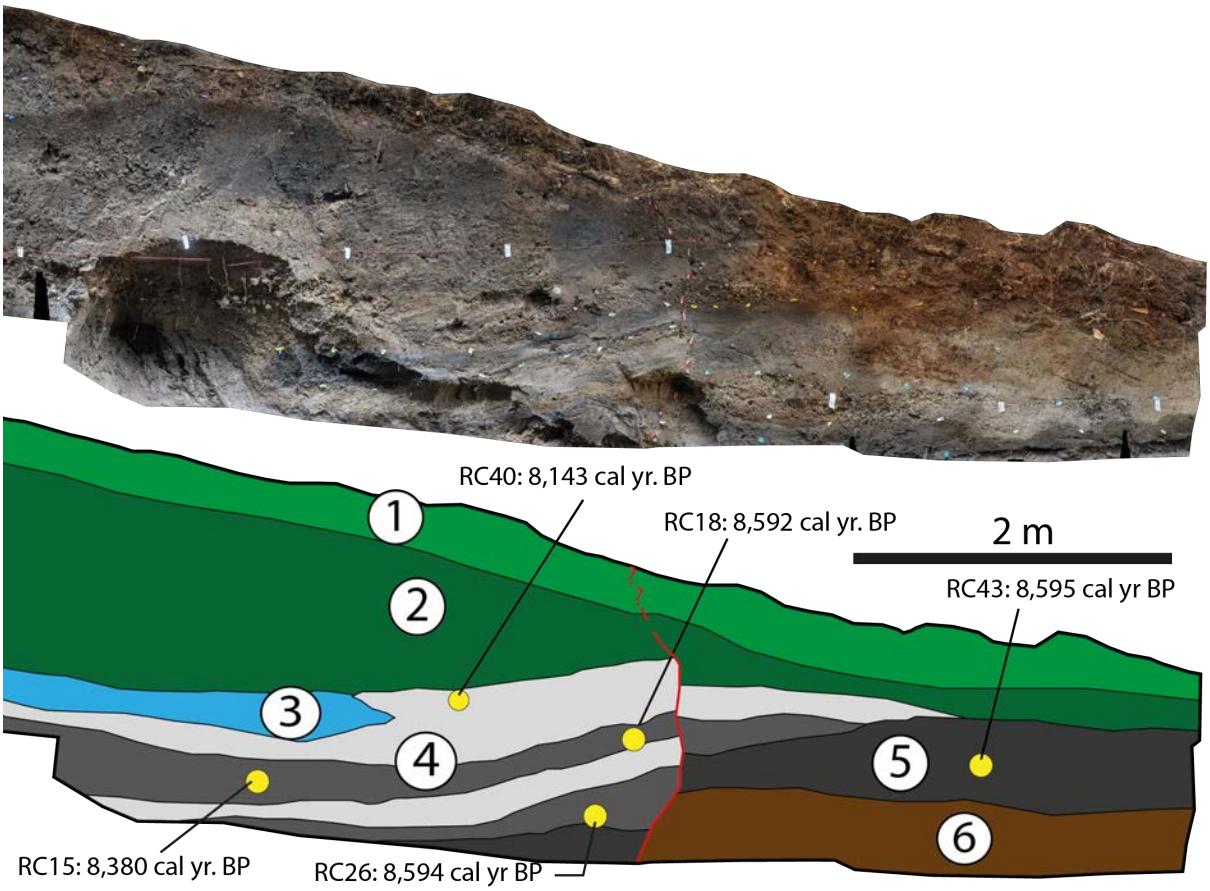


**Figure 7.** *Orthophotomosaic and stratigraphic log of the west wall of trench DV1 along the Dog Valley fault.*

**Age dating of sediments**

Table 1. Radiocarbon lab results and OxCal modeled ages for samples from the DV1 trench.

| Sample Name | Material | D14C | Radiocarbon Age (ybp) | Modeled Age (cal. ybp) |
|---|---|---|---|---|
| DVRC15 | Charcoal | -610.30 +/- 1.46 o/oo | 7570 +/- 30 | 8417-8343 |
| DVRC18 | Peat | -630.15 +/- 1.38 o/oo | 7990 +/- 30 | 8998-8655 |
| DVRC26 | Peat | -616.08 +/-1.43 o/oo | 7690 +/- 30 | 8543-8411 |
| DVRC40 | Peat | -599.98 +/- 1.49 o/oo | 7360 +/- 30 | 8310-8031 |
| DVRC43 | Wood | -613.68 +/- 1.44 o/oo | 7640 +/- 30 | 8520-8376 |

**Figure 8**. Field photograph showing sand dike that extends nearly to the ground surface.

**Discussion**

The Central and Northern Walker Lane from the Truckee region to near Mina, NV is composed of a series of northwest striking dextral strike-slip faults, northeast striking sinistral strike-slip faults, and north striking normal faults. Together these faults accommodate ~7 mm/yr of northwest directed dextral shear (Pierce et al., 2021). The Dog Valley fault likely plays a similar tectonic role in the Central/Northern Walker Lane as the similarly northeast oriented, left-lateral Wabuska, Carson, and Olinghouse faults (Li et al., 2017). These faults accommodate the opening of basins and block rotations that accommodate the overall northwest directed dextral shear of the Walker Lane (Pierce et al., 2021). Many of the large normal faults in the region appear structurally linked to these sinistral faults: the Genoa to the Carson fault, the Smith Valley fault to the Wabuska fault, and the Mt. Rose Fan fault zone to the Olinghouse fault. The Dog Valley fault continues this pattern and likely shares a similar structural relationship to the West Tahoe and Truckee fault zones.

Observations from trench DV1 along the Dog Valley fault indicate the occurrence of at least one earthquake that occurred after ~8,100 cal. ybp. that was associated with ~0.8 m of left-lateral displacement. Comparing this result to previously reported earthquake timing data from the conjugate Polaris fault indicates that the most recent earthquake along both faults post-dates ~7-8 ka (Melody et al., 2012). Although broadly constrained, the earthquake history allows the possibility that ruptures along each fault occurred closely spaced in time or possibly contemporaneously. Were both of these faults to rupture simultaneously during a single earthquake, the magnitude would be much greater than if each 20-30 km-long fault ruptured

independently. Our rupture mapping also indicates that at least a short part of the Dog Valley fault zone crosses the Polaris fault. Conjugate ruptures have occurred in several historical earthquakes both globally and in the Walker Lane (e.g. 2019 Ridgecrest; 2015 Nine-Mile Ranch; 1986 Chalfant Valley) and suggests that this style of strain release may be an underappreciated seismic hazard in the Walker Lane.

**Summary**

New lidar and field mapping identifies a clear Holocene rupture trace along ~20 km of the Dog Valley fault zone. Paleoseismic trenching confirms that an event with at least 80 cm of left-lateral displacement occurred after ~8,100 cal yr B.P.

**Topics for future work**

Additional trench sites should be selected to place younger limiting bounds on the timing of the earthquake identified in this study, to find evidence of earlier earthquakes, and to investigate the recurrence interval of this fault. A slip rate remains elusive for this fault, and if a suitable site can be found, geochronologic dating methods should be applied to measure the slip rate. Other faults in the Truckee Basin, including the Polaris & Truckee fault zones require further study to determine their rates of slip and earthquake histories.

**Reports Published**

This work has been published and presented in the 2021 AEG summer newsletter, 2021 Seismological Society of America annual meeting, and the 2021 PATA days conference proceedings. Citations for these presentations and publications are listed below. A manuscript is currently in preparation for peer-review and publication in the Bulletin of the Seismological Society of America.


Pierce, I., and Koehler, R.D., 2021, iPad lidar scanning for 3D trenching: a new methodology for paleoseismologists demonstrated on the Dog Valley fault, Truckee, CA, AEG News, Association of Environmental and Engineering Geologist, v. 64, no. 3, p. 29-32, Summer 2021.

Koehler, R.D., and Pierce, I., 2021, Distributed active faulting in the Truckee Basin, California, northern Walker Lane USA, Proceedings of the 10th International INQUA meeting on paleoseismology, active tectonics, and archaeoseismology (PATA), November 2021, Atacama Desert, Chile.

Pierce, I., and Koehler, R.D., 2021, New paleoseismic data demonstrate Holocene activity along the Dog Valley Fault, Truckee, CA, Seismological Society of America annual meeting, Seismological Research Letters, v. 92, no. 2B, p. 1338.


**Acknowledgements**


We are grateful for discussions in the field with T. Dawson, G. Seitz, J. Zachariasen, J. Bormann, J. McNeil, K. Adams, and K. Knudsen, and assistance from R. Arrowsmith in reconstructing the trench model. Research supported by U.S. Geological Survey (G20AP00055). Any use of trade, firm, or product names is for descriptive purposes only and does not imply endorsement by the U.S. Government. The views and conclusions contained in this Final Technical Report are those of the authors and should not be interpreted as necessarily representing the official policies, either expressed or implied, of the US Government.

**References**


Bormann, J.M., Hammond, W.C., Kreemer, C., Blewitt, G., 2016. Accommodation of missing shear strain in the Central Walker Lane, western North America: Constraints from dense GPS measurements. Earth Planet. Sci. Lett. 440, 169–177. https://doi.org/10.1016/j.epsl.2016.01.015

Bormann, J.M., Hammond, W.C., Kreemer, C., Blewitt, G., Jha, S., 2013. A Synoptic Model of Fault Slip Rates in the Eastern California Shear Zone and Walker Lane from GPS Velocities for Seismic Hazard Studies. Presented at the 2013 Seismological Society of America Annual Meeting, Seismological Research Letters, Salt Lake City, UT, p. 323.

Gold, R.D., Briggs, R.W., Personius, S.F., Crone, A.J., Mahan, S.A., Angster, S.J., 2014. Latest Quaternary paleoseismology and evidence of distributed dextral shear along the Mohawk Valley fault zone, northern Walker Lane, California. J. Geophys. Res. Solid Earth 119, 5014–5032. https://doi.org/10.1002/2014jb010987

Hammond, W.C., Blewitt, G., Kreemer, C., 2011. Block modeling of crustal deformation of the northern Walker Lane and Basin and Range from GPS velocities. J. Geophys. Res. 116. https://doi.org/10.1029/2010JB007817

Hatem, A.E., Collett, C.M., Gold, R.D., Briggs, R.W., Angster, S.A., Field, E.H., Anderson, M., Ben-Horin, J.Y., Dawson, T., DeLong, S., DuRoss, C., Thompson Jobe, J., Kleber, E., Knudsen, K.L., **Koehler, R.**, Koning, D., Lifton, Z., Madin, I., Mauch, J., Morgan, M., Pearthree, P., Petersen, M., Pollitz, F., Scharer, K., Powers, P., Sherrod, B., Stickney, M., Wittke, S., and Zachariasen, J., 2021, Earthquake geology inputs for the National Seismic Hazard Model (NSHM) 2023, version 1.0: U.S. Geological Survey data release, https://doi.org/10.5066/P918XCUU.

Hunter, L.E., Howle, J.F., Rose, R.S., Bawden, G.W., 2011. LiDAR-Assisted Identification of an Active Fault near Truckee, California. Bull. Seismol. Soc. Am. 101, 1162–1181. https://doi.org/10.1785/0120090261

Li, X., Huang, W., Pierce, I.K.D., Angster, S.J., Wesnousky, S.G., 2017. Characterizing the Quaternary expression of active faulting along the Olinghouse, Carson, and Wabuska lineaments of the Walker Lane. Geosphere 13, 2119–2136. https://doi.org/10.1130/GES01483.1

Melody, A.D., Whitney, B.B., Slack, C.G., 2012. Late Pleistocene and Holocene Faulting in the Western Truckee Basin North of Truckee, California. Bull. Seismol. Soc. Am. 102, 2219–2224. https://doi.org/10.1785/0120110260

OpenTopography, 2017. 2014 USFS Tahoe National Forest Lidar. https://doi.org/10.5069/G9V122Q1

Petersen MD, Moschetti MP, Powers PM et al. 2014. Documentation for the 2014 update of the United States National Seismic Hazard Maps. U.S. Geological Survey Open-File Report. 2014-1091, 243 pp.

Pierce, I.K.D., Wesnousky, S.G., Owen, L.A., 2017. Terrestrial cosmogenic surface exposure dating of moraines at Lake Tahoe in the Sierra Nevada of California and slip rate estimate for the West Tahoe Fault. Geomorphology 298, 63–71. https://doi.org/10.1016/j.geomorph.2017.09.030

Pierce, I.K.D., Wesnousky, S.G., Owen, L.A., Bormann, J.M., Li, X., Caffee, M., 2021. Accommodation of Plate Motion in an Incipient Strike-Slip System: The Central Walker Lane. Tectonics 40, e2019TC005612. https://doi.org/10.1029/2019TC005612

Reed, T.H., 2014. Spatial Correlation of Earthquakes with Two Known and Two Suspected Seismogenic Faults, North Tahoe-Truckee Area, California. M.S. thesis, Baylor University, 95 p.

Sylvester, A.G., Raines, G.L., 2013. Geology of the Independence Lake and Hobart Mills 7.5' Quadrangles, Nevada and Sierra Counties, California. California Geological Survey Map Sheet 63, scale 1:24,000.

## Appendices

### Appendix 1. Unit descriptions for stratigraphic deposits exposed in the trench.

| Unit # | Lower Contact | Upper Contact | Grain Size | Color | Description |
|---|---|---|---|---|---|
| 1 | Wavy/ gradual | n/a | Silt & sand | Gray/ brown | Surface soil, A horizon from soil description. Meadow environment w/ grass. |
| 2 | Sharp, wavy | Wavy/ gradual | Sandy silt to clayey-silt w/ gravel | Gray, brown w/ orange mottling | Trace subrounded cobbles up to 5 cm. Generally massive. Crude defined layers. Contains channel stringers of gravelly sand. Stringers of gravel have rounded pebbles up to 3 cm. Some crude layers of darker organic layers. |
| 3 | Sharp, semi-Planar/semi-wavy. | Sharp, Wavy | Rounded-subrounded cobbles up to 15 cm, gravel, sand, silt | Dark brown | Sandy silt loam matrix. Sometimes clast, sometimes matrix supported. Clasts are mostly white volcanics. Clasts average 3-6cm. |
| 4 | Sharp/ inter-bedded | Sharp, wavy | Silt & clay w/ interbedded sand lenses | black | Very sticky, very dark black, soft, abundant decomposed organics. From top to bottom, organic silt, interbedded clean sand, prominent organic silt at base. Sand interbed: gray/brown, clean sand. Single-grain, mostly med. gray sand. |
| 5 | | Wavy/ sharp | Sandy gravelly silt | gray brown | Massive unit, weak bedding. Base part has more gravel. |
| 6 | sharp | sharp | Very fine sand with rare cobbles | Beige | Massive beige very fine sand. Lenses of coarser sand and scattered cobble/gravel stringer lenses. |

**Appendix 2. Soil descriptions from the east wall of the trench.**

1) Depth: 0-15 cm. bottom contact transition is over 2cm. A. Texture: silt loam. Structure: 2 f & m sbk. Gravel <10%. Dry Consistence: Firm & Hard. Moist Consistence: Slightly Sticky (ss), slightly plastic. No clay films. Boundaries: c, w. Dry color: 10yr4/1 // dark gray. Moist color: 10yr2/1 // black. Notes: few fine, few medium roots.

2) Depth: 15-32 cm. bottom contact transition is over 4 cm. Bw1. Texture: Silty clay loam. Structure: 3, mc, sbk/abk. Gravel 10%. Dry consistence: Very Hard. Moist consistence: very firm. Clay films: v1, f, pf. Lower boundary: gradual, wavy. Dry Color: 10yr4/1 dark gray. Moist color: 10yr 2/1, black. Notes: roots are trace coarse, few medium.

3) Depth: 32-52 cm. bottom contact transition is over 3 cm. Bw2. Texture: silty clay loam. Structure: 3, m-c, sbk. Gravel 10-25%. Dry consistence: hard, very firm. Moist consistence: ss/ps. Clay films: v1, f, pf. Lower boundary: wavy, gradual. Dry Color: 10yr4/1 dark gray. Moist color: 10yr2/2 v. dark brown. Notes: roots are trace, medium.

4) Depth: 52-71 cm. bottom contact transition is over 2 cm. Bt(2Bt?). Texture: clay loam. Structure: 2 f-m sbk. Gravel <10%. Dry consistence: soft. Moist consistence: friable-very friable. Clay films: 2pf po. Lower boundary: wavy, abrupt. Dry color: 10yr4/2, dark grayish brown. Moist color: 10yr2/2, v. dark brown. Notes: few very fine pores, trace medium roots, orange mottling.

5) Depth: 71- 90+ cm. C/parent material. Texture: sandy loam. Visual color: dark brown-black.

**Appendix 3. Shapefile of Dog Valley fault traces**

A shapefile of the fault mapping line work can be downloaded at the link below. The Chrome browser works best. Paste the link into the browser and use the download tab at the bottom right of the screen.

https://github.com/lpslothman/fault/blob/4a1041ea14310894038130ef2786576785aa441b/DogValleyFlt.zip